Photoassisted Degradation of Dye Pollutants. V. Self-Photosensitized Oxidative Transformation of *Rhodamine B* under Visible Light Irradiation in Aqueous TiO_2 Dispersions

Taixing Wu, Guangming Liu, and Jincai Zhao*

Institute of Photographic Chemistry, Chinese Academy of Sciences, Beijing 100101, China

Hisao Hidaka

Frontier Research Center for the Earth Environment Protection, Meisei University, 2-1-1 Hodokubo, Hino, Tokyo 191, Japan

Nick Serpone

Department of Chemistry and Biochemistry, Concordia University, Montreal, Canada H3G 1M8

Received: January 28, 1998; In Final Form: April 27, 1998

Chemical oxygen demand (CODCr) and proton NMR, UV−vis, and spin trapping EPR spectroscopic evidence is presented to demonstrate the inverse photosensitized oxidative transformation of tetraethylated rhodamine (RhB) under visible illumination of aqueous titania dispersions. Both de-ethylation and oxidative degradation take place with the former proceeding in a stepwise manner to yield mono-, di-, tri-, and tetra-de-ethylated rhodamine species. Intermediates present after each de-ethylation step remain in a fast dynamic equilibrium between the titania particle surface and the bulk solution. The concentration of •OH radicals, formed from the inverse photosensitization process through the superoxide radical anion, increases upon addition of the anionic dodecylbenzene sulfonate surfactant (DBS) because a larger number of RhB excited states are able to inject an electron into the conduction band of the TiO_2 particles. Also, intermediates that can no longer absorb the visible light, (i.e., once the dye solution is competely bleached) are unable to drive the photosensitized degradation further. A mechanism for the competitive photoreactions between degradation and de-ethylation is described, in which de-ethylation $\{\zeta \sim 0.0035\}$ is mostly a surface occurring process, whereas degradation $\{\zeta \sim 0.0015\}$of the RhB chromophore is predominantly a solution bulk process.

Introduction

The semiconductor TiO_2 has proven to be an excellent photocatalyst material on which many organic substrates have been shown to be oxidatively (in some cases reductively) degraded and ultimately mineralized completely under UV irradiation.[1−12] In some cases, a plausible photocatalytic pathway has been inferred from the nature of the intermediates formed. The photocatalytic mechanism implicating titania particulates is now generally and reasonably well understood, although some aspects are still under debate.[3,8] Scheme 1A summarizes some of the accepted features of this *photocatalytic pathway*. Typically, after activation of the TiO_2 particles by UV light at wavelengths shorter than 385 nm (the absorption edge, band gap 3.2 eV for the anatase polymorph) and after various other events, electrons at the particle surface are scavenged by the ubiquitously present molecular oxygen to yield first the superoxide radical anion, $O_2^{\bullet -}$, whence on protonation yields the HOO• radical, whereas the valence band holes (redox potential ca. 2.9 eV vs NHE at pH 3) become trapped as the surface-bound •OH radicals on oxidation of either the surface OH^- groups and/or the surface H_2O molecules. The •OH radical

SCHEME 1: Comparison of the Photocatalytic Mechanism (A) for UV Irradiation of TiO_2 Particles with the Self-Photosensitized Pathway (B) under Visible Light Illumination

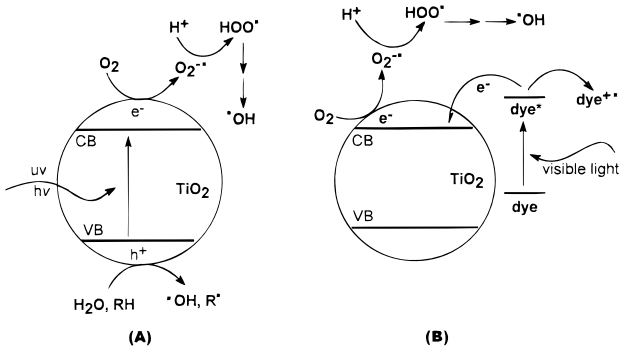

can also be formed from the trapped electron after formation of the HOO• radical by the sequence of reactions 1 and 2.

$$e^- + {}^\bullet OOH + H^+ \rightarrow H_2O_2 \qquad \text{(formation of } H_2O_2\text{)} \quad (1)$$

$$H_2O_2 + e^- \rightarrow {}^\bullet OH + OH^- \qquad \text{(formation of } {}^\bullet OH \text{ radicals)} \quad (2)$$

* To whom correspondence should be addressed. Fax: +86-10-6487-9375.

S1089-5647(98)00922-5 CCC: $15.00
Published on Web 07/03/1998

Photooxidation of the organic substrate RH (i.e., the rhodamine B dye (or the corresponding R$^{\bullet}$ radical from above)) by this mechanism can take place through reaction 3:

$$\text{RH or R}^{\bullet} + \{O_2, O_2^{\bullet-}, \text{HOO}^{\bullet}, \text{or } {}^{\bullet}\text{OH}\} \rightarrow \text{peroxy or hydroxylated...}$$

$$\text{intermediates} \rightarrow \rightarrow \text{degraded or mineralized products} \quad (3)$$

The active oxygen species $O_2^{\bullet-}$, HOO$^{\bullet}$, or $^{\bullet}$OH radicals have been implicated, with the latter radical more so, in the degradation of various organic substrates.[13,14] Hence, the *photocatalytic method* is an attractive candidate for treating organically polluted waters, and some success in this direction has been achieved.[15] However, the method is not without some limitations in its practical application because of the necessity for actinic UV-light, which is neither conveniently available (except during sunlight hours) nor inexpensive (if artificial) to use in activating the photocatalyst.

Dyes absorb visible light radiation and represent some of the principal pollutants in the textile and photographic industry. Whereas TiO_2 particles are not excited by visible light, dyes or analogous organic substrates can be, which under suitable energetics of the conduction band of TiO_2 and of the excited state of the dye, either ^{1}dye* and/or ^{3}dye*, leads to electron injection from the adsorbed ^{1,3}dye* species to the TiO_2 conduction band (and/or surface states). The injected electron reacts with the surface-adsorbed O_2 molecules to yield the $O_2^{\bullet-}$ radical anion and subsequently the HOO$^{\bullet}$ radical by protonation, in competition with back electron transfer to the dye$^{+\bullet}$ radical cation (see Scheme 1B). However, the latter option is usually some two to 3 orders of magnitude slower. Formation of $^{\bullet}$OH radicals follows the same path as in reactions 1 and 2, followed by a reaction sequence equivalent to those of eq 3, namely,

$$\text{Dye}_{ads}^{\bullet+} + \{{}^{\bullet}\text{OOH}, {}^{\bullet}\text{OH or } O_2\} \rightarrow \text{peroxides or hydroxylated...}$$

$$\text{intermediates} \rightarrow \rightarrow \text{degraded or mineralized products} \quad (4)$$

In this *photosensitization pathway*, the dye self-sensitizes its own oxidative transformation by the indirect formation of the oxidizing $^{\bullet}$OH radicals. The existence of TiO_2 particles is a prerequisite and play the important role of electron carriers to electron acceptors adsorbed on the particles. Consequently, the photodegradation of the dye induced by visible light might be more advantageous than that by UV radiation because more of the sunlight can be used during daylight hours, a significant economic advantage. Research in exploiting the self-photosensitization method to treat wastewaters has been rather scarce[16−19] as many of the reported studies have focused more on the details of the electron-transfer process per se.[20−22] Evidence that dyes can be degraded in this manner originates with this electron-transfer process from excited dyes to semiconductor particles.

In previous studies, we reported some work on the degradation of dyes illuminated by visible light radiation and photoassisted by TiO_2 particles.[23−25] However, photodegradation of the cationic Rhodamine B dye as the target pollutant in aqueous media, and in particular the degradation pathway mediated by TiO_2 particles under visible radiation have not been heretofore examined in much detail. The temporal self-photosensitized transformation of rhodamine B was monitored by UV−vis, ^{1}H nuclear magnetic resonance (NMR), and DMPO spin-trapping electron paramagnetic resonance (EPR) spectroscopies, as well as by chemical oxygen demand (as CODCr) measurements, to explore the nature of the active oxygen species, the nature of the intermediates and some of the details in an otherwise complex process.

Experimental Section

Materials. Titania particulates (P25, ca. 80% anatase, 20% rutile; BET area, ca. 50 m^2g^{-1}) were kindly supplied by Degussa Co. The 5,5-dimethyl-1-pyrroline-*N*-oxide (DMPO) was purchased from the Sigma Chemical Co.; rhodamine B (tetraethylrhodamine, RhB), sodium dodecylbenzene sulfonate (DBS), and other chemicals were of analytical reagent grade and used without further purification. For experiments involving Fe^{3+} and Cu^{2+} cations, we used $Fe_2(SO_4)_3$ and $CuSO_4$, respectively. Deionized and doubly distilled water was used throughout this study. For reference, the structure of RhB is shown below; the small letters identify the protons for NMR purposes.

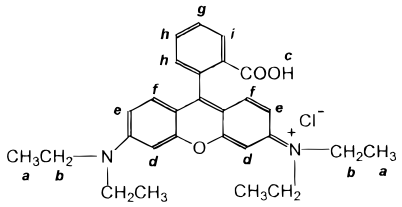

Rhodamine B

Photoreactor and Light Source. A 500-Watt halogen lamp (Institute of Electric Light Source, Beijing) was positioned inside a cylindrical Pyrex vessel; it was surrounded by a recirculating water jacket (Pyrex) to cool the lamp. An appropriate cutoff filter was placed outside the Pyrex jacket to completely remove wavelengths shorter than 420 nm and to ensure that irradiation was achieved by the visible light wavelengths only.

Procedures and Analyses. An aqueous TiO_2 dispersion was prepared by adding 100 mg of TiO_2 powder to a 50 mL solution containing the rhodamine B at appropriate concentrations. Prior to irradiation, the dispersions were magnetically stirred in the dark for ca. 30 min to secure the establishment of an adsorption/desorption equilibrium. At given irradiation time intervals, the dispersion was sampled (4 mL), centrifuged, and subsequently filtered through a Millipore filter (pore size, 0.22 μm) to separate the TiO_2 particles. The filtrates were analyzed by UV−vis spectra with a Shimadzu-160A spectrophotometer. Chemical oxygen demand (COD) measurements were carried out by the dichromate titration method[26] (referred to as CODCr) using two different but otherwise equivalent procedures: in the first, CODCr values were obtained after removal of TiO_2 particulates by filtration with the Millipore filter; in the second method, the CODCr values were obtained by direct measurements in the TiO_2 suspensions. The proton NMR spectra were obtained by Varian 300 nuclear magnetic resonance spectroscopy during the photodegradation of RhB. The samples for proton NMR spectra were prepared as follows: several aqueous dispersions of RhB (200 mL, 2×10^{-4} M) and TiO_2 (400 mg) were irradiated at different time intervals and TiO_2 particles were removed as described in the above method; the H_2O in the filtrates were removed (below 323 K) under the reduced pressure, and the remaining residues were dissolved in 0.5 mL $CDCl_3$ for NMR measurement. Electron paramagnetic resonance signals of radicals spin-trapped by DMPO were recorded with a Brucker EPR 300E spectrometer.

Photoefficiencies {here symbolized, ζ}of de-ethylation and degradation of the rhodamine B dye were determined at 560

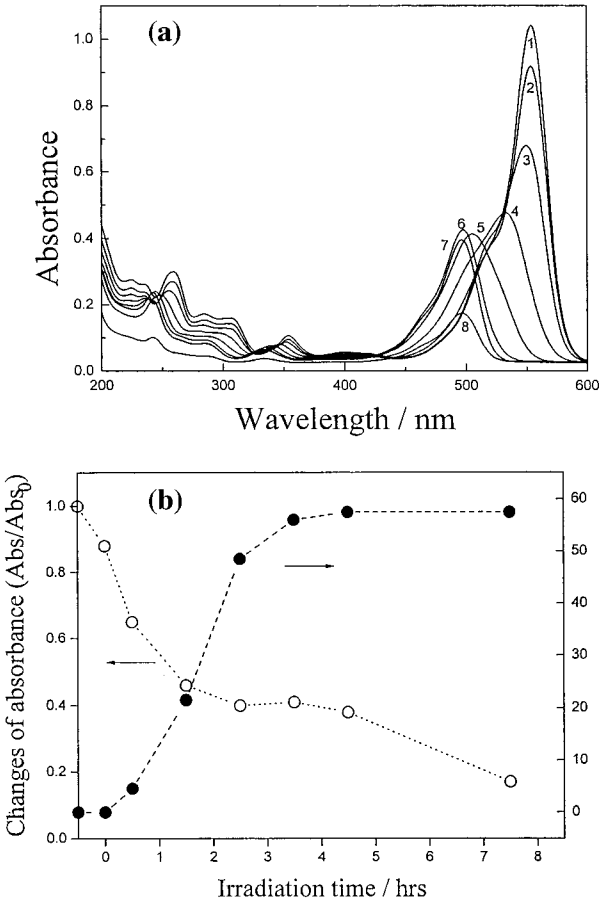

Figure 1. (a) UV−vis spectral changes of RhB (1×10^{-5} M, pH 4.2) as a function of irradiation time; spectra 2, 3, 4, 5, 6, 7, and 8 denote the irradiation times 0, 0.5, 1.5, 2.5, 3.5, 4.5, and 7.5 h, respectively. Spectrum 1 is the UV−vis spectrum of RhB before addition of TiO_2 particulates to the solution. (b) Absorbance changes in the major absorption band (empty circles) and the corresponding wavelength shifts (solid circles) of the spectra of (a).

nm using a Japan Optical Co. interference filter which cutoff wavelengths below 550 nm and above 570 nm. The photon fluence of the 500 watt halogen lamp at 560 nm was 1.3×10^{-8} einstein s^{-1} using the Reinickate actinometer (0.01 M, 50 mL, $\Phi = 0.27$).[27] For de-ethylation and degradation processes in the RhB/TiO_2 system, conditions were [RhB] $= 1 \times 10^{-5}$ M, 50 mL dispersion, TiO_2 loading, 100 mg. In the presence of the DBS surfactant at the cmc concentration of 1.2 mM and in which only degradation of the chromophore takes place (see below) conditions were [RhB] $= 1 \times 10^{-4}$ M, 50 mL dispersion, and TiO_2 loading, 100 mg. For the system, only an approximate photoefficiency was estimated owing to the complexity of the dispersion matrix.

Results and Discussion

The temporal evolution of the spectral changes taking place during the photosensitized degradation of RhB mediated by TiO_2 particles under visible irradiation is displayed in Figure 1a. Tetra-ethylated rhodamine, RhB, shows a major absorption band at 552 nm (spectrum 1). In the presence of TiO_2 particulates, the absorbance decreases by ca. 12% (spectrum 2), reflecting the extent of adsorption of RhB on titania in the dark. Visible light irradiation ($\lambda \geq 420$ nm) of the aqueous RhB/TiO_2 dispersion leads to a decrease in absorption with a concomitant wavelength shift of the band to shorter wavelengths, reminiscent of similar hypsochromic shifts seen by Watanabe et al [28] in the

SCHEME 2: Model Depicting the Fast Dynamic Equilibrium of RhB and the De-ethylated Rhodamine Species between the Solution Bulk and the TiO_2 Particle Surface during the Self-Photosensitized Transformation of RhB; RhB_1, RhB_2, etc., Refer to Mono-De-Ethylated and Bi-De-Ethylated Rhodamines

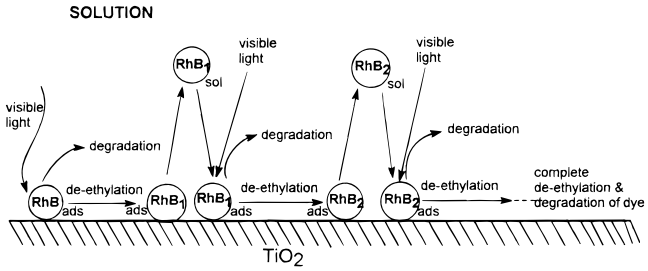

RhB/CdS system illuminated at $\lambda > 540$ nm. The trend in the blue shifts is illustrated in Figure 1b, which also depicts the overall diminution of the absorbance with increasing irradiation time.

Control experiments carried out on an aqueous RhB solution containing no TiO_2 particulates and on a RhB/TiO_2 dispersion in the dark, under otherwise identical experimental conditions, showed that in the absence of TiO_2 illumination of the RhB solution leads to no changes in absorption peak intensity and no peak wavelength shifts with increasing illumination time. No spectral changes were seen for the RhB/TiO_2 dispersion in the dark either; visible light illumination of RhB in the presence of SiO_2/Al_2O_3 particulates also led to no degradation of the dye[28] indicating the need for a semiconductor electron-transfer mediator {either CdS [28] or TiO_2}.

The wavelength shift depicted in Figure 1 is caused by de-ethylation of RhB because of attack by one of the active oxygen species on the *N*-ethyl group (see below). The earlier work on the RhB/CdS system[28] inferred a primary step in which the electron from the singlet excited state ^{1}RhB* to CdS particles came from the nitrogen atoms. Examination of the spectral variations of Figure 1a and the temporal behavior of Figure 1b suggests that RhB is de-ethylated in a stepwise manner (i.e., ethyl groups are removed one by one as confirmed by the gradual peak wavelength shifts toward the blue region (see Scheme 2)). De-ethylation of the fully *N*,*N*,*N*′,*N*′-tetraethylated rhodamine molecule (i.e., RhB) has the wavelength position of its major absorption band moved toward the blue region, λ_{max}, RhB, 552 nm; *N*,*N*,*N*′-tri-ethylated rhodamine, 539 nm; *N*,*N*′-di-ethylated rhodamine, 522 nm; *N*-ethylated rhodamine, 510 nm; and rhodamine, 498 nm; the molar extinction coefficient ϵ_{max} lies in the range $5-12 \times 10^4$ $M^{-1}cm^{-1}$.[28] From the ϵ_{max} data, the fully de-ethylated rhodamine species should have a peak intensity at 498 nm ca. 70% of that of the fully tetra-ethylated rhodamine (RhB) species assuming that the conjugated ring structure (see above) is not destroyed. In fact, the actual peak intensity of the rhodamine at 498 nm is less (∼40% between 1.5 and 4.5 h of irradiation) than that of Rhodamine B for equal concentrations of the initial rhodamine molecule. Wavelength shifts of the major absorption band are no longer observed after ca. 4 h of irradiation, Figure 1b.

The above results are analogous to those of the competitive photodegradation reactions between the polyoxyethylene chain and the aromatic ring in polyoxyethylated nonylphenol.[29] During the initial period of photodegradation of RhB, competitive reactions between de-ethylation and cleavage of the RhB chromophore ring structure occur, with de-ethylation predominating. Irradiation by visible light for longer times leads to

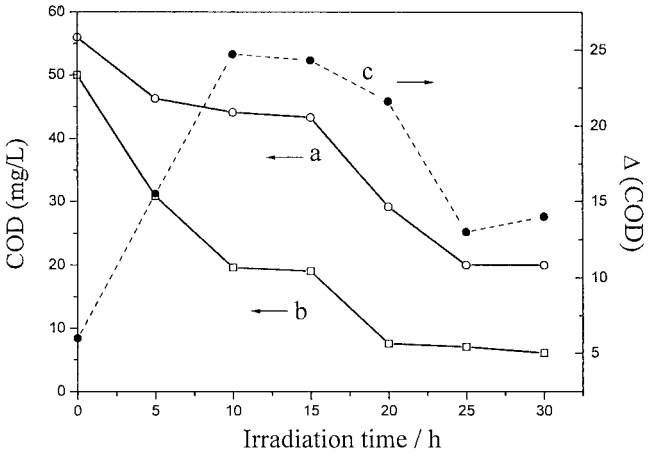

Figure 2. Chemical oxygen demand (as CODCr; see text) data for RhB (5×10^{-5} M, pH 4.0) versus irradiation time. Curve a: CODCr of the entire suspensions. Curve b: CODCr of the bulk solution after removal of the TiO_2 particles. Curve c represents the difference [curves a and b] and reflects the quantity of rhodamine B and the various intermediates adsorbed on the TiO_2 particulates.

further decomposition of the de-ethylated rhodamine intermediates as indicated by changes in peak intensity at 498 nm (Figure 1a). Photoefficiencies for de-ethylation and degradation are, respectively, $\zeta = 0.0035$ and $\zeta = 0.0015$.

Chemical oxygen demand (CODCr) values reflect the general concentration of organics in the solution bulk, and therefore changes in CODCr mirror the degree of degradation or mineralization of an organic substrate during the irradiation period. CODCr values (Figure 2) of both the irradiated RhB/TiO_2 suspensions (curve a) and of the bulk solution after removal of TiO_2 (curve b) decrease with increasing illumination time. The CODCr values of the dispersion (curve a) are greater than those of the bulk solution (curve b), showing that there must be a considerable quantity of RhB, de-ethylated RhB or some other intermediate species adsorbed on the surface of the TiO_2 particles. Moreover, during the 5−15 h irradiation period, the difference in CODCr values between those of the dispersion and those of the bulk solution increase with an increase in irradiation time, reflecting the increase in the amount of organic species being adsorbed on the TiO_2 surface. In the 15−25 h period, Δ{CODCr} decreases, inferring that the intermediate species also degrade with further illumination,[24] after which the temporal evolution of CO_2 is inhibited as the dispersion becomes totally discolored (bleached). These observations support the self-photosensitization mechanism (Scheme 1B) proposed earlier.[23−25]

The temporal profile of the changes taking place in the RhB chromophore was also monitored by proton NMR spectroscopy (Figure 3). Spectrum a illustrates the proton NMR signals of pure RhB and the related assignments of the various proton chemical shifts (see structure of RhB above). As the degradative changes evolve (spectra a−e of Figure 3), a sequence of new signals appear at δ 9.0−9.5, 3.0, 2.7−1.7, and 1.5−1.3 ppm (−CH_3 and analogous groups) while the characteristic signals of RhB at δ 3.55 ppm (−CH_2−) and δ 8.3−6.6 ppm (aromatic protons) disappear. Of particular relevance are the single peak at δ 9.0−9.5 ppm (new), the single peak at δ 3.05 ppm (new), and the methylene (−CH_2−) peak at δ 3.55 ppm which exhibit special changes: the first two signals increase with irradiation time, whereas the latter signal decrease. Moreover, the single peak seen at $\delta \sim 9.0$ ppm after 18 h of irradiation shifts to lower field (ca. 9.5 ppm) with increasing illumination time to

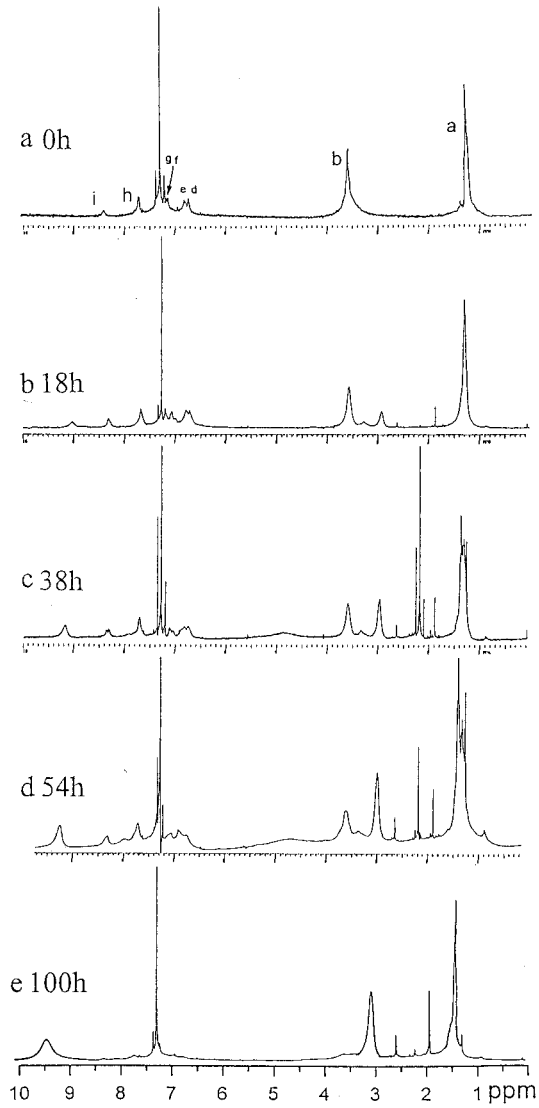

Figure 3. Temporal proton NMR spectral profiles of the changes occurring during the degradation of RhB at different irradiation times. {the strong signal at δ 7.3 ppm is that of $CHCl_3$ present in deuterated chloroform, see Experimental Section}.

100 h. We attribute this signal to the aldehyde proton of CH_3-CHO,[28] although we cannot preclude the presence of CH_3-COOH. These NMR findings indicate that both de-ethylation and degradative changes in the aromatic chromophore take place concurrently, although de-ethylation appears to dominate during the initial irradiation period. Ultimately, the chromophoric structure of RhB also degrades (cf. Schemes 2 and 3) consistent with the results of Figure 1a.

The RhB/DBS/TiO_2 system (DBS is the dodecylbenzene sulfonate surfactant) was examined by DMPO spin-trapped EPR spectroscopy to monitor the radicals that form during the photosensitized degradation process. The results summarized in Figure 4 show the signature of the DMPO−•OH adduct on irradiating this RhB/DBS/TiO_2 dispersion with visible radiation; the EPR signal intensity increases in the first 8 min of irradiation and decays subsequently. At 15 min of irradiation, the signal of the DMPO−•OH species is barely discernible. By comparison with the EPR results from the RhB/TiO_2 suspensions examined earlier,[25a] two significant results emanate from the EPR observations in Figure 4: (i) the concentration of the DMPO−•OH adduct formed in the RhB/DBS/TiO_2 dispersions is greater than the concentration of the adduct formed during

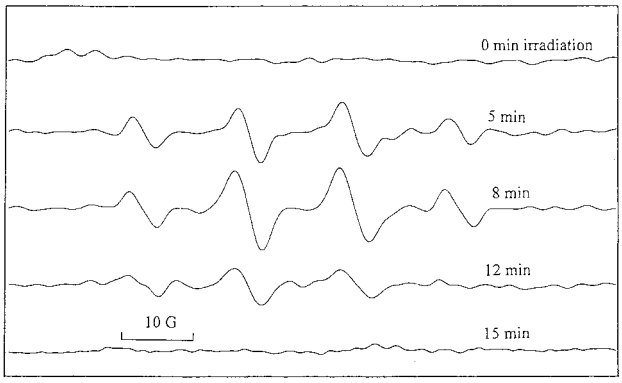

Figure 4. EPR spectral changes of the DMPO−•OH adduct with increasing irradiation time in the RhB (2×10^{-4} M, pH 3.8)/DBS-(cmc)/TiO_2 (2 g L^{-1}) dispersions.

SCHEME 3: Formation and Competitive Reactions of •OH Radicals under Different Conditions during Visible Light Irradiation of Rhodamine B. (a) RhB/TiO_2 Dispersion System; (b) RhB/Cu^{2+}/TiO_2 Dispersion System; (c) H_2O_2/Fe^{3+}/RhB Homogeneous System

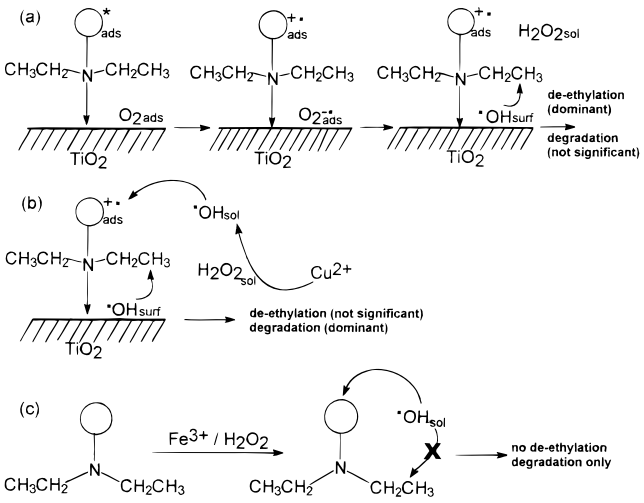

illumination of the RhB/TiO_2 system, and (ii) its lifetime is longer (ca. 12 min). In the latter system, the signals of the DMPO−•OH adduct were weaker and the lifetime was less than 3 min, under otherwise similar experimental conditions. We deduce that •OH radicals participate in the photosensitized degradation of RhB, that the anionic DBS surfactant enhances the adsorption of the cationic dye RhB on the TiO_2 surface allowing for a larger number of excited RhB* molecules to inject electrons into the TiO_2 particles, and that, as a result, generates a greater quantity of •OH radicals (see eqs 1,2), thereby increasing the rate of degradation of RhB by influencing reaction 4 $\{\zeta \approx 0.0091\}$.

Additional supporting evidence for the self-photosensitization pathway (Scheme 1B) emerges from an examination of the Cu^{2+}/RhB/TiO_2 heterogeneous system (Figure 5) and the H_2O_2/Fe^{3+}/RhB system in homogeneous media (Figure 6). By contrast with the data of Figure 1 in which the rate of degradation of RhB and the ephemeral peak wavelength shifts are relatively rapid, the data of Figure 5 suggest a slower change in peak wavelength shift and a slower rate of de-ethylation than those seen for the RhB/TiO_2 dispersions. However, the data of Figure 6 indicate only a decrease in absorbance with irradiation time and no peak wavelength shifts for the H_2O_2/Fe^{3+}/RhB system. We deduce that there is no de-ethylation of RhB

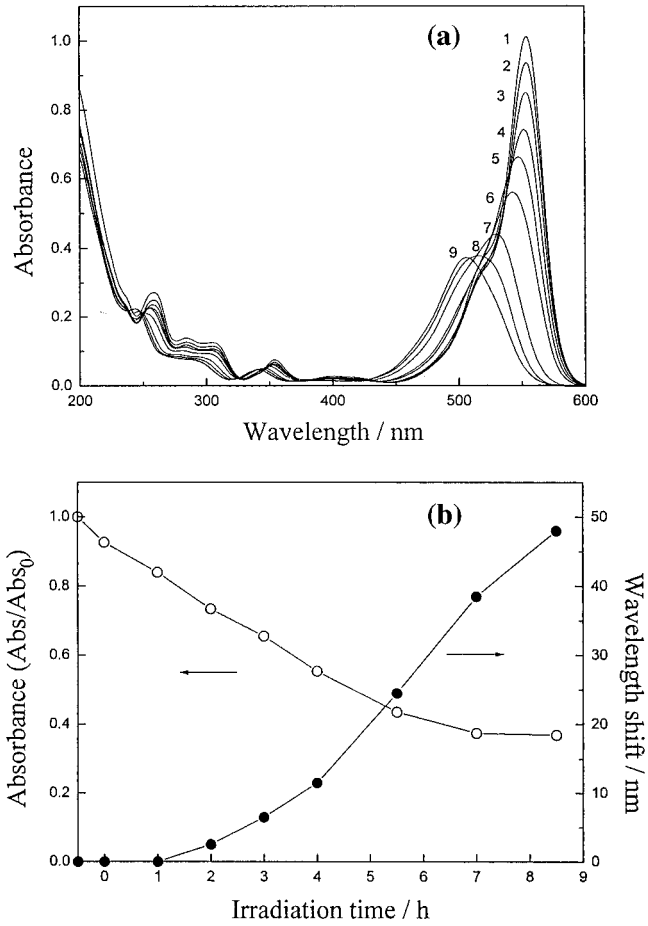

Figure 5. (a) UV−vis spectral changes of RhB (1×10^{-5} M, pH 4.2) as a function of irradiation time (1 h interval) on addition of Cu^{2+} (3×10^{-4} M) to the RhB/TiO_2 heterogeneous system. Spectrum 1 is the corresponding spectrum before addition of TiO_2 and spectra 2, 3, 4, 5, 6, 7, 8, and 9 denote irradiation for 0, 1, 2, 3, 4, 5, 6, and 7 h, respectively. (b) Absorbance changes (empty circles) and wavelength shifts (solid circles) under the same conditions as in (a).

in this case and that only degradation of the aromatic chromophore takes place relatively rapidly in less than ca. 90 min.

The Fe^{3+}/H_2O_2 system can also produce •OH radicals through reactions 5−7:[30,31]

$$Fe^{3+} + H_2O_2 \rightarrow Fe^{2+} + {}^{\bullet}OOH + H^+ \quad (5)$$

$$Fe^{3+} + {}^{\bullet}OOH \rightarrow Fe^{2+} + O_2 + H^+ \quad (6)$$

$$Fe^{2+} + H_2O_2 \rightarrow Fe^{3+} + {}^{\bullet}OH + OH^- \quad (7)$$

The •OH radicals produced by these reactions (or equivalent) have been observed by the DMPO−•OH adduct signature in an EPR experiment (not shown). Consequently, the results of Figure 6 emanate principally from an attack of the chromophoric structure of RhB by •OH radicals in homogeneous media and not from an •OH attack on the ethyl groups (Scheme 3c). However, according to eqs 1, 3, and 4, hydrogen peroxide and organic peroxides are formed in RhB/TiO_2 dispersions on visible irradiation; •OH radicals are formed subsequently in reaction 2 by electron reduction of H_2O_2. These peroxides tend to have a lower activity than •OH radicals and do not degrade the RhB dye efficiently (as tested by an experiment involving only RhB and H_2O_2 in aqueous media, confirming the earlier observations by Watanabe and co-workers[28]); note that hydrogen peroxide desorbs to the solution bulk. Thus, when Cu^{2+} is added to the

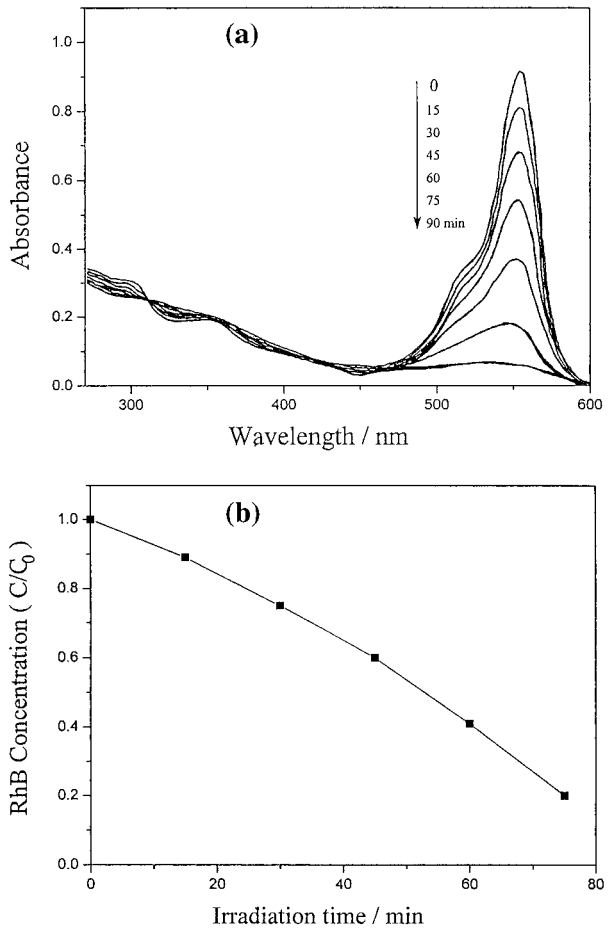

Figure 6. (a) UV−vis spectral changes of RhB (1×10^{-5} M, pH 4.2) with irradiation time (interval, every 15 min) for the H_2O_2/Fe^{3+}/RhB system in homogeneous media; (b) normalized concentration changes versus irradiation time. {Note the isosbestic point at ca. 310 nm during the entire irradiation period in (a)}.

RhB/TiO_2 dispersions, reactions analogous to eqs 5−7 can take place and produce •OH radicals[32−34] in the solution bulk (Scheme 3b), which also attack RhB but principally at the aromatic chromophore leading to the degradation of the RhB structure rather than to de-ethylation (Figure 6).

The temporal changes in absorbance exhibit good linear relationships for the data in Figures 5 and 6, at least for the first 5.5 h and 50 min of irradiation, respectively, in contrast to the data of Figure 1. This presumes some distinct similarities in the chemistries of the Cu^{2+}/RhB/TiO_2 and Fe^{3+}/H_2O_2/RhB systems. To the extent that •OH radicals produced in the solution bulk can be chemisorbed rapidly by the TiO_2 particulates in the heterogeneous system,[35] in competition with reaction with RhB, de-ethylation of the fully *N*,*N*,*N*′,*N*′-tetraethylated rhodamine species is mainly a surface occurring reaction, whereas degradation of RhB by •OH radicals is predominantly a solution bulk process. Degradation is slow on the TiO_2 surface relative to de-ethylation.

Conclusions

Both de-ethylation and degradation of RhB take place in the presence of TiO_2 particles under visible light irradiation. De-ethylation predominates during the initial irradiation period, as confirmed by proton NMR spectral evidence in that the proton signals of the $-CH_3$ group change first and ultimately the proton signals of the aromatic ring disappear. De-ethylation of RhB takes place in a stepwise manner with the various de-ethylated intermediate rhodamine species remaining in equilibrium between the TiO_2 surface and the bulk solution. Addition of the anionic surfactant DBS to the RhB/TiO_2 dispersions results in an increase of •OH radicals. De-ethylation of RhB by •OH radicals is mostly a surface occurring process whereas oxidative degradation of the dye chromophore predominates in solution. From a practical and economic perspective, the self-photosensitized degradation of colored dyes by visible light radiation might in some cases be preferable to the UV-photocatalytic pathway. Degradation of dye pollutants can be driven by sunlight during daylight hours and at other times by the more economical (than UV) artificial lamps that emit visible radiation.

Acknowledgment. The authors appreciate the generous financial support of this work from the National Natural Science Foundation of China (Grants 29677019 and 29725715) and the Foundation of the Chinese Academy of Sciences and the China National Committee for Science and Technology to J.Z., by a Grant-in-Aid for Scientific Research from the Ministry of Education (Grant 10640569) to H. H., and by the Natural Sciences and Engineering Research Council of Canada (Grant A5443) to N.S. We are also grateful to Prof. J. Chen for measurements of the EPR spectra and thank a referee for bringing ref 19 to our attention.

References and Notes

(1) Bahnemann, D. F.; Cunningham, J.; Fox, M. A.; Pelizzetti, E.; Pichat, P.; Serpone, N. In *Aquatic and Surface Photochemistry*; Helz, G., Zepp, R. G., Crosby, D. G., Eds.; Lewis Publishers: Boca Raton, FL., 1994; pp 261−316.

(2) Fox, M. A.; Dulay, M. T. *Chem. Rev.* **1993**, *93*, 341.

(3) Heller, A. *Acc. Chem. Res.* **1995**, *28*, 503.

(4) Ollis, D. F., Al-Ekabi, H. Eds. *Photocatalytic Purification and Treatment of Water and Air*; Elsevier Science Publishers: Amsterdam, 1993.

(5) Ollis, D. F.; Pelizzetti, E.; Serpone, N. *Environ. Sci. Technol.* **1991**, *25*, 1523.

(6) Serpone, N. In *Water Purification by Photocatalytic, Photoelectrochemical, and Electrochemical* Processes; The Electrochemical Society: Bennington, N. J., 1994; Vol. 94, p 236.

(7) Mills, A.; Le Hunte, S. *J. Photochem. Photobiol. A* **1997**, *108*, 1.

(8) (a) Linsebigler, A. L.; Lu, G.; Yates, J. T., Jr., *Chem. Rev.* **1995**, *95*, 735. (b) Fan, J.; Yates, J. T., Jr. *J. Am. Chem. Soc.* **1996**, *118*, 4686.

(9) Serpone, N., Pelizzetti, E., Eds. "*Photocatalysis−Fundamentals and Applications*; Wiley-Interscience: New York, 1989.

(10) Kamat, P. V. *Chem. Rev.* **1993**, *93*, 267.

(11) Hoffmann, M. R.; Martin, S. T.; Choi, W.; Bahnemann, D. W. *Chem. Rev.* **1995**, *95*, 69.

(12) (a) Hidaka, H.; Nohara, K.; Zhao, J.; Pelizzetti, E.; Serpone, N. *J. Photochem. Photobiol. A* **1995**, *91*, 145. (b) Hidaka, H.; Horikoshi, S.; Ajiaka, K.; Zhao, J.; Serpone, N. *J. Photochem. Photobiol. A* **1997**, *108*, 197. (c) Hidaka, H.; Zhao, J.; Pelizzetti, E.; Serpone, N. *J. Phys. Chem.* **1992**, *96*, 2226.

(13) Jaeger, C. D.; Bard, A. *J. Phys. Chem.* **1979**, *83*, 3146.

(14) Izumi, I.; Fan, F.-R. F.; Bard, A. *J. Phys. Chem.* **1981**, *85*, 218.

(15) For example, see: Blake, D. M. *Bibliography of Work on the Heterogeneous Photocatalytic* Removal of Hazardous Compounds from Water and Air (update No. 2 to October 1996). Report No. NREL/TP-430-22197; National Renewable Energy Laboratory; Golden, CO, Jan 1997.

(16) Hagfeldt, A.; Graetzel, M. *Chem. Rev.* **1995**, *95*, 49.

(17) Parkinson, B. A.; Splitler, M. T. *Electrochim. Acta* **1992**, *37*, 943.

(18) Vinodgopal, K.; Wynkoop, D. E.; Kamat, P. V. *Environ. Sci. Technol.* **1996**, *30*, 1660.

(19) Ross, H.; Bendig, J.; Hecht, S. *Sol. Energy Mater. Sol. Cells* **1994**, *33*, 475.

(20) Rossetti, R.; Brus, L. E. *J. Am. Chem. Soc.* **1984**, *106*, 4336.

(21) Vinodgopal, K.; Kamat, P. V. *J. Photochem. Photobiol. A* **1994**, *83*, 141.

(22) He, J.; Zhao, J.; Shen, T.; Hidaka, H.; Serpone, N. *J. Phys. Chem.* **1997**, *101*, 9027.

(23) Zhang, F.; Zhao, J.; Zang, L.; Shen, T.; Hidaka, H.; Pelizzetti, E.; Serpone, N. *J. Mol. Catal. A* **1997**, *120*, 173.

(24) Zhang, F.; Zhao, J.; Shen, T.; Hidaka, H.; Pelizzetti, E.; Serpone, N. *Appl. Catal. B* **1998**, *15*, 147.

(25) (a) Qu, P.; Zhao, J.; Shen, T.; Hidaka, H. *J. Mol. Catal. A* **1998**, *129*, 257. (b) Zhao, J.; Wu, K.; Wu, T.; Hidaka, H.; Serpone, N. *J. Chem.*

Soc., Faraday Trans. **1998**, *94*, 673. (c) Zhao, J.; Wu, T.; Wu, K.; Oikawa, K.; Hidaka, H.; Serpone, N. *Environ. Sci. Technol.* In press.

(26) Chinese National Standard. GB 11914−89; **1989**.

(27) Wegner, E. E.; Adamson, A. W. *J. Am. Chem. Soc*. **1966**, *88*, 394.

(28) (a) Watanabe, T.; Takizawa, T.; Honda, K. *J. Phys. Chem*. **1977**, *81*, 1845. (b) Inoue, T.; Watanabe, T.; Fujishima, A.; Honda, K.; Kohayakawa, K. *J. Electrochem. Soc*. **1977**, *124*, 719.

(29) Pelizzetti, E.; Minero, C.; Maurino, V.; Sclafani, A.; Hidaka, H.; Serpone, N. *Environ. Sci. Technol*. **1989**, *23*, 1380.

(30) Walling, C. H. *Acc. Chem. Res*. **1975**, *8*, 125.

(31) Barb, W. G.; Baxendale, J. H.; George, P.; Hargrave, K. R. *Trans. Faraday Soc*. **1951**, *47*, 591.

(32) Fujihira, M.; Satoh, Y.; Osa, T. *Bull. Chem. Soc. Jpn*. **1982**, *55*, 666.

(33) Ito, S.; Kunai, A.; Okada, H.; Sasaki, K. *J. Org. Chem.* **1988**, *53*, 296.

(34) Wei, T.; Wang, Y.; Wan, C. *J. Photochem. Photobiol. A* **1990**, *55*, 115.

(35) Lawless, D.; Serpone, N.; Meisel, D. *J. Phys. Chem*. **1991**, *95*, 5166.